The 2010 IEEE/RSJ International Conference on
Intelligent Robots and Systems
October 18-22, 2010, Taipei, Taiwan

Efficient Pulling Motion of a Two-Link Robot Arm near Singular Configuration

Takateru Urakubo, Tomoaki Mashimo and Takeo Kanade

Abstract— **This paper discusses the advantages of singular configurations of a two-link robot arm in achieving tasks of pulling or lifting a heavy object. Optimal base location and arm motion for minimizing the joint torques are examined by numerical simulations, and the base location where the robot arm is near a singular configuration at the start time of task is optimal. It is shown analytically that joint torques can supply energy to the system composed of the robot arm and the object efficiently near singular configurations of the arm. The energy supply rates at two singular configurations are derived based on the equations of motion of the system.**

I. INTRODUCTION

Lifting or pulling a heavy object is a physically strenuous task for humans. The robots are expected to do such tasks in behalf of us [1]. To reduce the energy consumption, the tasks should be done as efficiently as possible. A mobile manipulator would serve as a robot that helps us at home in near future. It can utilize the motion of both the mobile base and the manipulator to achieve the tasks. The problem of planning the motion has attracted the attention of many researchers [2], [3]. But, even if the mobile base is fixed during a task, we can choose the base location at the start time and the motion of the arm during the task. The latter problem is simpler than the former one, and thereby we can examine in detail the features of the dynamics of the system composed of the arm and the object for the latter problem. In this paper, we deal with the problem of finding the optimal base location and arm motion for a two-link robot arm, and investigate an important feature of the dynamics near singular configurations of the arm. The feature would be also applicable to solving more complicated problems.

Singular configurations of a robot arm are the postures where the manipulability of the robot arm is degenerated [4], that is, the kinematic mapping between *joint space* and *task space* is singular. For a two-link robot arm, there are two singular configurations, where the robot arm is stretched out or folded completely. The motion planning of the robot arm through the singular configurations is difficult, because the velocity vector of the end effector is restricted in a certain direction. Several methods to solve the difficulty have been proposed by using a time scale transformation and so on [5], [6]. In many studies on motion planning, it is common to avoid the singular configurations because of the undesirable feature of the kinematics [7]. On the other hand, how is the dynamics of the robot arm affected by the kinematic feature of singular configurations? The dynamic manipulability proposed in [8] measures the acceleration of the end effector, that is, the acceleration in task space. In the statics, a robot arm can sustain a large load by small joint torques near a singular configuration [9]. In [10], joint torques that are necessary to generate an end effector motion along the singular direction is specified. In [11], we have examined the optimal base location and arm motion of a two-link robot arm for door opening task, and have shown that the base location where the robot arm is almost stretched out at both the start and end of door opening is optimal for a sufficiently heavy door.

In this paper, we consider the problem of pulling or lifting a heavy object by a two-link robot arm. The cost function for optimization is chosen as the integral of squared joint torques during the task. When the object is heavy, a large amount of energy is needed to achieve the task. The energy is supplied to the system composed of the robot arm and the object by the product of joint torques multiplied by joint angle displacements. In that sense, dynamic features of the system in joint space are very important to the achievement of the task. We examine the acceleration of joint angles generated by joint torques in detail and show that the torques can supply energy most efficiently at singular configurations for a sufficiently heavy object. Although both of two singular configurations of a two-link robot arm have an advantage in supplying energy, the supply rate at the configuration where the robot arm is stretched out is better than at the configuration where the robot arm is folded completely. For the door opening task in [11], we could see the advantage of singular configurations clearly, because the position of the end effector is restricted on the path of a door knob and the primary role of joint torques is to supply or absorb energy. For the tasks of pulling or lifting a heavy object, the joint torques have to not only supply energy but also control the position of the object. Nevertheless, numerical simulation results show that the configuration of the robot arm at the start time of the task is almost singular at the optimal base location. The feature of the dynamics near singular configurations is useful for achieving the tasks.

II. PROBLEM FORMULATION

We suppose that a two-link robot arm grabs a heavy weight, and pulls or pushes it to the desired position. The following assumptions are made for simplicity;

1) The location of the robot base can be chosen at the start time, and it is fixed during the task.
2) There are no frictions at the joints of the robot arm.

T. Urakubo is with Department of Systems Science, Kobe University, Nada-ku, Kobe 657-8501, Japan urakubo@cs.kobe-u.ac.jp

T. Mashimo and T. Kanade are with the Robotics Institute, Carnegie Mellon University, Pittsburgh, PA 15213, USA

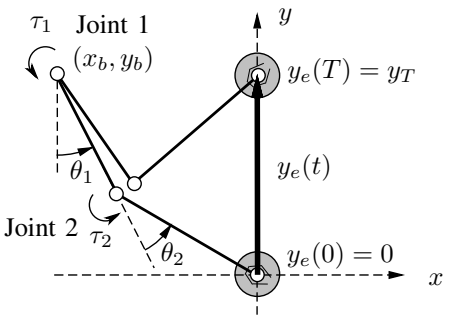

Fig. 1. Two-link robot arm with a weight

3) The weight can be modeled as a mass point.
4) The weight is made to be moved along a straight line from the initial position to the desired position.

There are infinite number of paths of the weight that connect an initial position to a final position. The desirable paths are different depending on the tasks and the environments such as obstacles. In this paper, we choose a simple path, a straight line, as in the assumption 4). When the weight is sufficiently heavy, the straight line would be a reasonable path in the absence of obstacles.

A. Two-Link Robot Arm

As shown in Fig. 1, the joint between the robot base and the first link of the arm is called Joint 1, and the joint between the first link and second link of the arm is called Joint 2. We introduce a coordinate frame, (x, y), whose origin is placed on the initial position of the weight, and the y axis is set to be along the path to the desired position. The location of the robot base is denoted as $\boldsymbol{p}_b = [x_b, y_b]^T$, and the angles of Joint 1 and 2 are denoted as θ_1 and θ_2 respectively. The input torques at Joint 1 and 2 are expressed as τ_1 and τ_2 respectively. The angles and the torques are represented in vector forms as $\boldsymbol{\theta} = [\theta_1, \theta_2]^T$ and $\boldsymbol{\tau} = [\tau_1, \tau_2]^T$. We summarize the inverse kinematics and dynamics of the system below.

Denoting the position of the end effector of the robot arm as $\boldsymbol{p}_e = [x_e, y_e]^T$, we can express it by using joint angles $\boldsymbol{\theta}$.

$$\boldsymbol{p}_e = \boldsymbol{f}(\boldsymbol{\theta}) = \begin{bmatrix} x_b + l_1 \sin\theta_1 + l_2 \sin(\theta_1 + \theta_2) \\ y_b - l_1 \cos\theta_1 - l_2 \cos(\theta_1 + \theta_2) \end{bmatrix} , \quad (1)$$

where l_1 and l_2 are the lengths of the first and second links respectively. When the trajectory of the end effector $\boldsymbol{p}_e(t)$ is given for $0 \le t \le T$, we can obtain two points of $\boldsymbol{\theta}$ for each time t as long as $\theta_2 \neq k\pi$ (k is an integer). To get a unique solution of $\boldsymbol{\theta}$, we choose one of them that satisfies $\theta_2 \ge 0$ at $t = 0$. For $t > 0$, θ_2 is chosen so that $\dot{\theta}_2$ is continuous. From (1), we can obtain the following equations:

$$\dot{\boldsymbol{p}}_e = \boldsymbol{J}\dot{\boldsymbol{\theta}} , \ \ddot{\boldsymbol{p}}_e = \boldsymbol{J}\ddot{\boldsymbol{\theta}} + \dot{\boldsymbol{J}}\dot{\boldsymbol{\theta}} , \quad (2)$$

where $\boldsymbol{J}$ is the Jacobian matrix of $\boldsymbol{f}$ and can be written as

$$\boldsymbol{J} = \begin{bmatrix} l_1 \cos\theta_1 + l_2 \cos(\theta_1 + \theta_2) & l_2 \cos(\theta_1 + \theta_2) \\ l_1 \sin\theta_1 + l_2 \sin(\theta_1 + \theta_2) & l_2 \sin(\theta_1 + \theta_2) \end{bmatrix} . \quad (3)$$

By using (2), we can obtain $\dot{\boldsymbol{\theta}}$ and $\ddot{\boldsymbol{\theta}}$ from $\boldsymbol{p}_e(t)$ as long as $\det(\boldsymbol{J}) \neq 0 \Leftrightarrow \theta_2 \neq k\pi$.

The equations of motion of a two-link robot arm can be written in the following form:

$$\boldsymbol{\tau} = \boldsymbol{M}(\boldsymbol{\theta})\ddot{\boldsymbol{\theta}} + \boldsymbol{h}(\boldsymbol{\theta}, \dot{\boldsymbol{\theta}}) + \boldsymbol{\tau}_g(\boldsymbol{\theta}) + \boldsymbol{J}^T\boldsymbol{F} , \quad (4)$$

where the kinetic energy of the two-link arm can be expressed as $E_a = (1/2)\dot{\boldsymbol{\theta}}^T\boldsymbol{M}(\boldsymbol{\theta})\dot{\boldsymbol{\theta}}$ by using $\boldsymbol{M}(\boldsymbol{\theta})$, and $\boldsymbol{h}$ can be expressed as $\boldsymbol{h} = \dot{\boldsymbol{M}}(\boldsymbol{\theta})\dot{\boldsymbol{\theta}} - (\partial E_a/\partial\boldsymbol{\theta})^T$. The term $\boldsymbol{\tau}_g(\boldsymbol{\theta})$ is derived from the potential energy of the arm $P_a(\boldsymbol{\theta})$ as $\boldsymbol{\tau}_g = (\partial P_a(\boldsymbol{\theta})/\partial\boldsymbol{\theta})^T$, and $\boldsymbol{F} = [F_1, F_2]^T$ is the force applied to the weight by the robot hand. From the equations of motion of the weight, $\boldsymbol{F}$ can be written as

$$m_w\ddot{\boldsymbol{p}}_e = \boldsymbol{F} , \quad (5)$$

where m_w is the mass of the weight. From (2), (4) and (5), we can obtain

$$\boldsymbol{\tau} = (\boldsymbol{M}(\boldsymbol{\theta}) + m_w\boldsymbol{J}^T\boldsymbol{J})\ddot{\boldsymbol{\theta}} + \boldsymbol{h}(\boldsymbol{\theta}, \dot{\boldsymbol{\theta}}) + m_w\boldsymbol{J}^T\dot{\boldsymbol{J}}\dot{\boldsymbol{\theta}} + \boldsymbol{\tau}_g(\boldsymbol{\theta}) , \quad (6)$$

When the trajectories of joint angles, $\boldsymbol{\theta}(t)$, are given from the inverse kinematics, the trajectories of joint torques, $\boldsymbol{\tau}(t)$, can be calculated from (6).

B. Optimal Base Location and Arm Motion

In this paper, we examine the optimal base location and arm motion of the two-link robot arm in two cases: *Case A* and *Case B*. In Case A, each link of the robot arm rotates in a horizontal plane, and the weight is pulled or pushed horizontally. The external force $\boldsymbol{\tau}_g$ in (6) is zero in this case. In Case B, each link of the robot arm rotates in a vertical plane, and the weight is lifted up vertically. In both cases, the initial and final positions of the weight are set to be $\boldsymbol{p}_e = [0, 0]^T$ and $\boldsymbol{p}_e = [0, y_T]^T$ respectively. Note that the y axis is horizontal in Case A and vertical in Case B. We consider a trajectory that connects those two positions along y axis as in Fig. 1, and denote it as $\boldsymbol{p}_e(t) = [0, y_e(t)]^T$. The conditions on $y_e(t)$ at the start time, $t = 0$, and the end time, $t = T$, are given as follows:

$$(y_e, \dot{y}_e)|_{t=0} = (0, 0) \ \ , \ \ (y_e, \dot{y}_e)|_{t=T} = (y_T, 0) . \quad (7)$$

We introduce the following cost function as a criterion for optimization.

$$J_c(\xi) = \int_{t=0}^{T} (\tau_1^2 + \tau_2^2)dt , \quad (8)$$

where ξ represents the parameters for optimization. It is chosen for each case as follows.

Case A: $\xi = \{\boldsymbol{p}_b, y_e(t)\}$, Case B: $\xi = \{\boldsymbol{p}_b, y_e(t), T\}$.

In Case B, the end time of lifting up should be included in ξ. The value of the cost function highly depends on the end time because of the gravity term $\boldsymbol{\tau}_g$. In Case A, after scale transformations of time t and torque $\boldsymbol{\tau}$, we can choose the end time as $T = 1$ [s] without loss of generality. In this paper, we deal with an optimization problem of finding the parameters that minimize J_c:

$$\xi^* = \arg\min J_c . \quad (9)$$

III. Optimization Method

The main purpose of this paper is to show an advantage of singular configurations of the robot arm in achieving tasks. We do not have to find the optimal solution ξ^* that minimizes the cost function (8) rigorously. We approximate $y_e(t)$ as fifth order spline functions of time, and find the coefficients of splines that minimize the cost function. The location of the robot base (x_b, y_b) is discretized into a grid, and, at each grid point, the quasi-optimal motion of the weight is calculated by using the spline functions.

A. Search for optimal motion of weight

We divide the time interval $[0, T]$ by n and assume that the trajectory of $y_e(t)$ in each time interval $[t_i, t_{i+1}]$ ($i = 0, \cdots, n-1$ and $t_j = jT/n$ for $j = 0, \cdots, n$) is expressed by a fifth order polynomial function of time, $\varphi_i(t)$, as follows:

$$\begin{aligned}\varphi_i(t) \;=\; & y_i + b_i(t-t_i) + c_i(t-t_i)^2 + d_i(t-t_i)^3 \\ & + e_i(t-t_i)^4 + f_i(t-t_i)^5 \;, \end{aligned} \tag{10}$$

where y_i, b_i, c_i, d_i, e_i and f_i are scalar parameters. To make the input torque $\boldsymbol{\tau}$ continuous, we choose the functions $\varphi_i(t)$ such that $\varphi_i(t_{i+1}) = \varphi_{i+1}(t_{i+1})$, $\dot{\varphi}_i(t_{i+1}) = \dot{\varphi}_{i+1}(t_{i+1})$, $\ddot{\varphi}_i(t_{i+1}) = \ddot{\varphi}_{i+1}(t_{i+1})$, for $i = 0, \cdots, n-2$. When the polynomials satisfy those conditions and (7), there are $3n-1$ independent parameters, and they can be chosen as $\boldsymbol{\Phi} = (y_1, \cdots, y_{n-1}, e_0, f_0, \cdots, e_{n-1}, f_{n-1})$. We assume that $y_e(t)$ monotonically increases at $t = t_i$ and put a constraint that $0 \le y_1 \le \cdots \le y_{n-1} \le y_T$. At each location of the robot base, we search for the values of $\boldsymbol{\Phi}$ in Case A or $(\boldsymbol{\Phi}, T)$ in Case B that minimize the cost function (8), by the Quasi-Newton method.

B. Search for optimal location of robot base

The grid search method is used to find the optimal base location. The region of (x_b, y_b) defined by $[x_{\min}, x_{\max}] \times [y_{\min}, y_{\max}]$ is divided into a grid, where each rectangle is given by $\Delta x \times \Delta y$. By calculating the cost function at each grid point by the method in III-A, we can find the optimal location of the robot base.

IV. Numerical Simulations

In this section, we will show the optimal solution obtained by numerical simulations. To find the optimal values of $\boldsymbol{\Phi}$ or $(\boldsymbol{\Phi}, T)$, the MATLAB function fmincon was used. In both Case A and B, the displacement of the weight, y_T, is set to be 0.3 [m], and the time interval T is divided into four sub-intervals, that is, $n = 4$. The initial values of $\boldsymbol{\Phi}$ are given so that the initial spline curves coincide with a single third order spline curve that satisfies (7). The lengths of two links of the arm are chosen as $l_1 = 0.3$ [m] and $l_2 = 0.35$ [m]. Their mass and inertia are set to be 0.49 [kg], 0.12 [kg·m^2], 0.66 [kg] and 0.12 [kg·m^2] respectively.

Case A: Horizontal Motion

The mass of the weight is set to be 10.0 [kg], and the end time T is chosen as 1.0 [s]. At first, the grid points of (x_b, y_b) were made by choosing Δx and Δy as 0.05 [m], and the cost function J_c in (8) was calculated at each point. Figure 2 shows the contour plot of J_c. The contours are almost symmetrical with respect to the middle point of the path of the weight, $(0, 0.15)$. There exist two candidates of global minimum at the locations denoted as L_1 and L_2. The values of J_c at both locations are almost the same, and they are 5.03 [N^{2}m^{2}s]. Next, to obtain more accurate solution of the optimal location, the grid points near L_1 or L_2 were made by choosing Δx and Δy as 0.01 [m]. Figure 3 shows the contour plot of J_c near L_1, and the optimal location denoted as L_1' is $(x_b, y_b) = (0.06, 0.64)$. The value of J_c at L_1' is 4.34 [N^{2}m^{2}s]. The contour plot of J_c near L_2 is also similar to Fig. 3. The optimal location near L_2 is $(x_b, y_b) = (-0.06, -0.34)$, and the value of J_c is 4.34 [N^{2}m^{2}s], which is almost the same as the one at L_1'.

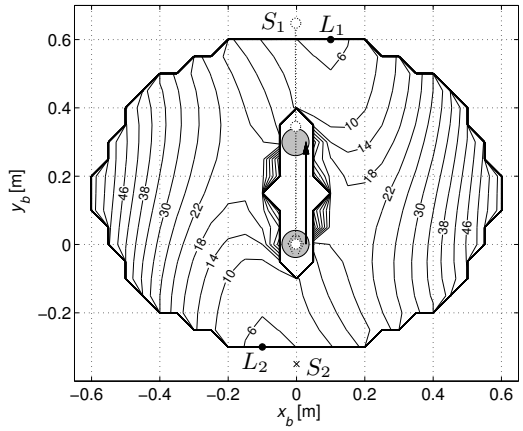

Fig. 2. Cost function for base location (x_b, y_b) (Case A)

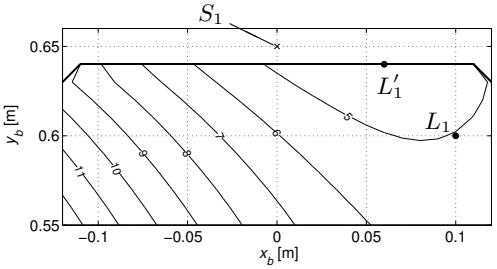

Fig. 3. Cost function for base location (x_b, y_b) near L_1 (Case A)

Here, we consider the locations denoted as S_1 and S_2 in Fig. 2 where $(x_b, y_b) = (0.0, 0.65)$ and $(x_b, y_b) = (0.0, -0.35)$ respectively. When the robot base is located at S_1, the robot arm is stretched out and aligned with the path of the weight at the start time as in Fig. 2, and the matrix $\boldsymbol{J}$ defined by (3) is degenerated. For the location S_2, the robot arm is stretched out at the end time. We call such a location *singular location* in this paper. It should be noted that the optimal locations obtained near L_1 and L_2 are close to the singular locations. Figures 4 and 5 show the time histories of $(y_e, \dot{y}_e, \ddot{y}_e)$ and $\boldsymbol{\tau}$ at the location L_1'. Around the start time, the arm pulls the weight to accelerate it near the singular configuration. The acceleration is larger than the deceleration around the end time, while the norms of the required torques around the start and end time are not so different.

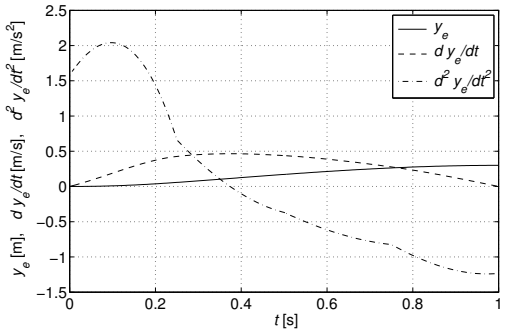

Fig. 4. Time history of weight position y_e at L_1' (Case A)

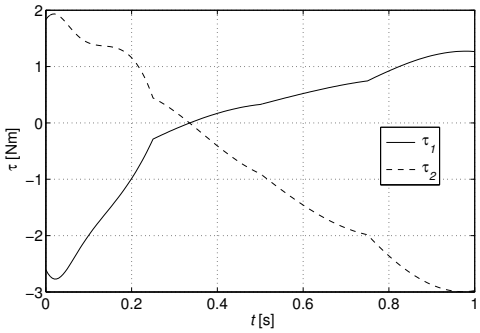

Fig. 5. Time history of joint torque $\boldsymbol{\tau}$ at L_1' (Case A)

Case B: Vertical Motion

The mass of the weight is set to be 5.0 [kg], and the initial value of T is chosen as 0.5 [s]. At first, the grid points of (x_b, y_b) were made by choosing Δx and Δy as 0.05 [m], and the cost function J_c was calculated at each point. Figure 6 shows the contour plot of J_c. The contours are not symmetrical because of the gravity. The location of the minimum of J_c is $(x_b, y_b) = (0.05, 0.6)$ and denoted as L_1. By choosing Δx and Δy as 0.01 [m] near L_1, we obtained more accurate solution of the optimal location as $(x_b, y_b) = (0.03, 0.64)$. The location is denoted as L_1' in Fig. 6, and the initial configuration of the robot arm at L_1' is also shown in the figure. The value of J_c at L_1' is 27.2 [N^{2}m^{2}s]. In Fig. 6, we can see that the cost function has a local minimum at the location denoted as L_2. The location is calculated as $(x_b, y_b) = (-0.09, -0.05)$ by using $\Delta x = \Delta y = 0.01$. The value of J_c at L_2 is 68.5 [N^{2}m^{2}s]. It should be noted that the initial configuration at L_2 is close to a singular configuration where the robot arm is folded completely, that is, $\theta_2 = \pi$.

V. Efficient Energy Supply near Singularity

In [11], we have shown that the singular configuration where $\theta_2 = 0$ is useful for providing energy to the system efficiently by joint torques. In this section, it will be shown that the singular configuration where $\theta_2 = \pi$ is also useful for that purpose, and the differences between the results in IV and those in [11] will be discussed.

A. Energy Supply

In this subsection, we consider only Case A for simplicity. It is supposed that the robot arm is in a singular configuration at the start time and pulls a weight horizontally. The singular

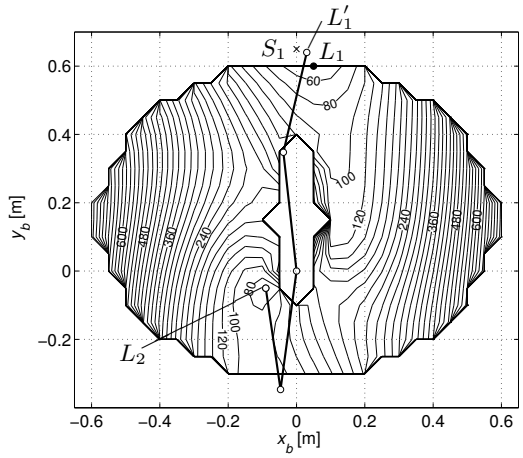

Fig. 6. Cost function for base location (x_b, y_b) (Case B)

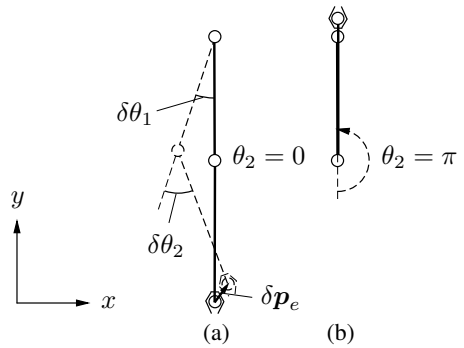

Fig. 7. Singular configurations. (a) $\mathcal{C}_0$: $\theta_2 = 0$. (b) $\mathcal{C}_\pi$: $\theta_2 = \pi$.

configuration shown in Fig. 7 (a) is denoted as $\mathcal{C}_0$, and the one in Fig. 7 (b) is denoted as $\mathcal{C}_\pi$. The small displacements of joint angles from each singular configuration are denoted as $\delta\boldsymbol{\theta}$, and the small displacement of the end effector caused by $\delta\boldsymbol{\theta}$ is denoted as $\delta\boldsymbol{p}_e$ (Fig. 7). To simplify the analysis, we make the following assumptions:

5) At the start time, the arm and the weight are at rest, and a bounded and constant torque $\boldsymbol{\tau}$ is applied at the joints for $t \geq 0$.
6) The mass of the weight is much larger than the mass and inertia of the robot arm.

The work done by joint torque can be written as $W_J = \boldsymbol{\tau}^T \delta\boldsymbol{\theta}$. In statics, it is equal to the energy supplied to the weight and can be represented as $W_J = \boldsymbol{F}^T \delta\boldsymbol{p}_e$ by using the force $\boldsymbol{F}$ applied to the weight. But, this equation means that an infinitesimal torque $\boldsymbol{\tau}$ can cause a finite force $\boldsymbol{F}$, and the statics is insufficient to explain the behavior of the system [11]. We consider the dynamics of the system below.

In Case A, (6) can be rewritten as

$$\ddot{\boldsymbol{\theta}} = \boldsymbol{P}(\boldsymbol{\tau} - \boldsymbol{h} - m_w \boldsymbol{J}^T \dot{\boldsymbol{J}} \dot{\boldsymbol{\theta}}) \ , \tag{11}$$

where

$$\boldsymbol{P} = (\boldsymbol{M} + m_w \boldsymbol{J}^T \boldsymbol{J})^{-1} \ . \tag{12}$$

Since $\dot{\boldsymbol{\theta}} = 0$ at the start time under the assumption 5), we can approximate $\ddot{\boldsymbol{\theta}}$ as

$$\ddot{\boldsymbol{\theta}} \approx \boldsymbol{P}\boldsymbol{\tau} \ . \tag{13}$$

The small displacement of $\boldsymbol{\theta}$ at $t = \delta t$ can be represented as $\delta\boldsymbol{\theta} \approx (\delta t^2/2)\boldsymbol{P}\boldsymbol{\tau}$, and the work done by joint torque $\boldsymbol{\tau}$ can be written as

$$W_J = \boldsymbol{\tau}^T \delta\boldsymbol{\theta} \approx (\delta t^2/2)\boldsymbol{\tau}^T \boldsymbol{P}\boldsymbol{\tau} \ . \tag{14}$$

Since $\boldsymbol{P}$ is symmetric, it can be expressed as

$$\boldsymbol{P} = \lambda_1 \boldsymbol{e}_{\lambda_1}\boldsymbol{e}_{\lambda_1}^T + \lambda_2 \boldsymbol{e}_{\lambda_2}\boldsymbol{e}_{\lambda_2}^T \ , \tag{15}$$

where $\boldsymbol{e}_{\lambda_i}$ is the normalized eigenvector for eigenvalue λ_i $(i = 1, 2)$ and $\boldsymbol{e}_{\lambda_1}^T \boldsymbol{e}_{\lambda_2} = 0$. From $\boldsymbol{P} > 0$, $\lambda_i > 0$ and we assume that $\lambda_1 \geq \lambda_2$. The work W_J can be maximized by choosing the joint torque as $\boldsymbol{\tau} \parallel \boldsymbol{e}_{\lambda_1}$:

$$W_J \approx (\delta t^2/2)\lambda_1 \|\boldsymbol{\tau}\|^2 \ , \text{ when } \boldsymbol{\tau} \parallel \boldsymbol{e}_{\lambda_1} \ . \tag{16}$$

Under the assumption 6), the eigenvalues can be calculated as follows:

$$\lambda_1 = \frac{2}{m_w(k_1 - \sqrt{k_1^2 - 4k_3}) + (a - \frac{ak_1 - 2k_2}{\sqrt{k_1^2 - 4k_3}}) + O(\frac{1}{m_w})} \ ,$$

$$\lambda_2 = \frac{2}{m_w(k_1 + \sqrt{k_1^2 - 4k_3}) + (a + \frac{ak_1 - 2k_2}{\sqrt{k_1^2 - 4k_3}}) + O(\frac{1}{m_w})} \ ,$$

where, denoting the i-j component of $\boldsymbol{M}$ as M_{ij} ($M_{12} = M_{21}$), $a = M_{11} + M_{22} > 0$,

$$k_1(\theta_2) = l_1^2 + 2l_2^2 + 2l_1 l_2 \cos\theta_2 > 0 \ , \tag{17}$$

$$\begin{aligned} k_2(\theta_2) \ &= \ M_{11}l_2^2 + M_{22}(l_1^2 + l_2^2 + 2l_1 l_2 \cos\theta_2) \\ &\quad -2M_{12}l_2(l_2 + l_1\cos\theta_2) \ , \end{aligned} \tag{18}$$

$$k_3 = l_1^2 l_2^2 (1 - \cos^2\theta_2) \ . \tag{19}$$

When the configuration of the robot arm is not singular, $\cos^2\theta_2 \neq 1$ and $k_3 > 0$. Then, both of λ_1 and λ_2 approach zero as $m_w \to \infty$. As a result, the work W_J approaches zero. The joint torque $\boldsymbol{\tau}$ cannot accelerate the joint angle $\boldsymbol{\theta}$, because the weight is too heavy. In other words, when the matrix $\boldsymbol{J}$ is not degenerated, W_J can be approximated as

$$W_J \approx (\delta t^2/2)\boldsymbol{\tau}^T (m_w \boldsymbol{J}^T \boldsymbol{J})^{-1} \boldsymbol{\tau} \equiv W_{J1} \ , \tag{20}$$

and $W_{J1} \to 0$ as $m_w \to \infty$.

When the configuration of the robot arm is singular, $\cos^2\theta_2 = 1$ and $k_3 = 0$. Then, only λ_2 approaches zero as $m_w \to \infty$, and λ_1 can be calculated as

$$\lambda_1 = k_1/k_2 + O(1/m_w) \ . \tag{21}$$

Since $\boldsymbol{e}_{\lambda_2}$ converges to the column space of $\boldsymbol{J}^T$ from (12) as $m_w \to \infty$, $\boldsymbol{e}_1$ satisfies $\boldsymbol{e}_{\lambda_1}^T \mathrm{col}(\boldsymbol{J}^T) \approx \boldsymbol{e}_{\lambda_1}^T \boldsymbol{e}_{\lambda_2} = 0$. Consequently, λ_1 and $\boldsymbol{e}_{\lambda_1}$ can be calculated for the singular configurations $\mathcal{C}_0$ and $\mathcal{C}_\pi$ respectively as follows.

• When the robot arm is in $\mathcal{C}_0$, that is, when $\cos\theta_2 = 1$,

$$\lambda_1 \approx \frac{\|\boldsymbol{c}_0\|^2}{\boldsymbol{c}_0^T \boldsymbol{M}\boldsymbol{c}_0} \equiv \lambda_{10} \ , \ \boldsymbol{e}_{\lambda_1} \approx \frac{\boldsymbol{c}_0}{\|\boldsymbol{c}_0\|} \ , \tag{22}$$

where $\boldsymbol{c}_0 = [l_2, -(l_1 + l_2)]^T$.

• When the robot arm is in $\mathcal{C}_\pi$, that is, when $\cos\theta_2 = -1$,

$$\lambda_1 \approx \frac{\|\boldsymbol{c}_\pi\|^2}{\boldsymbol{c}_\pi^T \boldsymbol{M}\boldsymbol{c}_\pi} \equiv \lambda_{1\pi} \ , \ \boldsymbol{e}_{\lambda_1} \approx \frac{\boldsymbol{c}_\pi}{\|\boldsymbol{c}_\pi\|} \ , \tag{23}$$

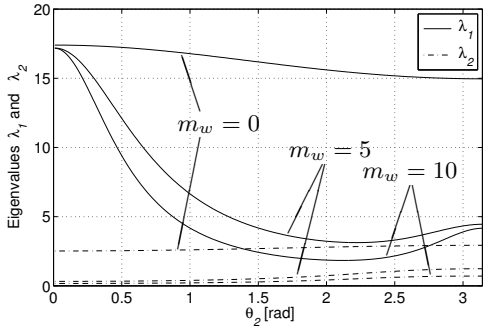

Fig. 8. Eigenvalues λ_1 and λ_2 of $\boldsymbol{P}$

where $\boldsymbol{c}_\pi = [l_2, l_1 - l_2]^T$.

Equations (22) and (23) mean that, when the matrix $\boldsymbol{J}$ is degenerated at $\mathcal{C}_\alpha$, the work W_J can be approximated as

$$W_J \approx \frac{\delta t^2}{2} \frac{(\boldsymbol{c}_\alpha^T \boldsymbol{\tau})^2}{\boldsymbol{c}_\alpha^T \boldsymbol{M}\boldsymbol{c}_\alpha} \ , \tag{24}$$

where $\alpha = 0$ or π. In order to maximize W_J, we can choose $\boldsymbol{\tau}$ as $\boldsymbol{\tau} \parallel \boldsymbol{c}_\alpha$ and obtain

$$W_J \approx \frac{\delta t^2}{2} \frac{\|\boldsymbol{c}_\alpha\|^2 \|\boldsymbol{\tau}\|^2}{\boldsymbol{c}_\alpha^T \boldsymbol{M}\boldsymbol{c}_\alpha} \equiv W_{J2_\alpha} \ , \text{ when } \boldsymbol{\tau} \parallel \boldsymbol{c}_\alpha \ . \tag{25}$$

From (20) and (25), we can see that $W_{J1} \ll W_{J2_\alpha}$ because of the assumption 6). Therefore, when m_w is large enough, the joint torque $\boldsymbol{\tau}$ can generate the energy most efficiently at the singular configurations. Moreover, by noting that $\boldsymbol{M}$ also depends on θ_2, it can be shown that $\boldsymbol{c}_0^T \boldsymbol{M}\boldsymbol{c}_0 = \boldsymbol{c}_\pi^T \boldsymbol{M}\boldsymbol{c}_\pi$. Therefore, we can obtain

$$\lambda_{10} > \lambda_{1\pi} \ , \tag{26}$$

from $\|\boldsymbol{c}_0\| > \|\boldsymbol{c}_\pi\|$, that is, $W_{J2_0} > W_{J2_\pi}$.

Figure 8 shows the variations in λ_1 and λ_2 as functions of θ_2 for $m_w = 0$, 5 and 10 [kg], where the physical parameters of the robot arm are the same as in IV. When $\theta_2 \neq 0$ or π, both eigenvalues decrease as m_w increases. But, λ_1 converges to a certain nonzero value when $\theta_2 = 0$ and π, which is consistent with (22) and (23).

B. Energy Flow

When the robot arm is in a singular configuration, the work W_J generated by $\boldsymbol{\tau}$ is not directly transmitted to the kinetic energy of the weight. From the assumption 5), (2) and (13), $\ddot{\boldsymbol{p}}_e$ can be approximated as $\ddot{\boldsymbol{p}}_e \approx \boldsymbol{J}\ddot{\boldsymbol{\theta}} \approx \boldsymbol{J}\boldsymbol{P}\boldsymbol{\tau} \approx \lambda_2 \boldsymbol{J}\boldsymbol{e}_{\lambda_2}\boldsymbol{e}_{\lambda_2}^T\boldsymbol{\tau}$, where we used that $\boldsymbol{J}\boldsymbol{e}_{\lambda_1} \approx 0$ at the singular location assuming that m_w is sufficiently large. A small increase of the energy of the weight, δE_w, can be approximated as

$$\delta E_w = m_w \lambda_2^2 \|\boldsymbol{J}\boldsymbol{e}_{\lambda_2}\boldsymbol{e}_{\lambda_2}^T\boldsymbol{\tau}\|^2 \delta t^2/2 = O(1/m_w) \to 0 \ ,$$

as $m_w \to \infty$. Therefore, even if $\boldsymbol{\tau}$ includes nonzero components along both $\boldsymbol{e}_{\lambda_1}$ and $\boldsymbol{e}_{\lambda_2}$, δE_w can be approximated as zero. When $\boldsymbol{\tau}$ includes a nonzero component along $\boldsymbol{e}_{\lambda_1}$, nonzero energy W_J is generated from (25), and it is stored in the robotic arm as the kinetic energy of the arm:

$$\delta E_a \approx W_J \ . \tag{27}$$

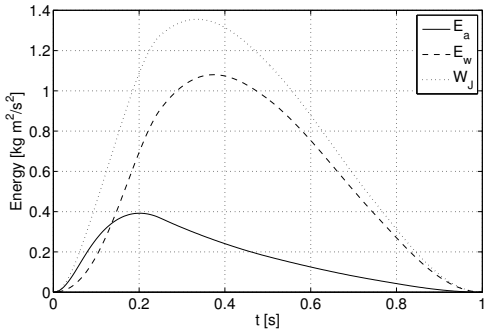

Fig. 9. Time histories of E_a, E_w and W_J at L_1' (Case A)

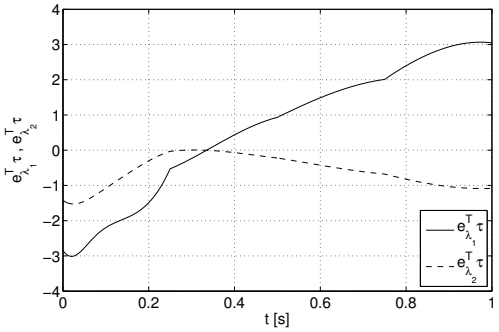

Fig. 10. Time histories of $\boldsymbol{e}_{\lambda_1}^T \boldsymbol{\tau}$ and $\boldsymbol{e}_{\lambda_2}^T \boldsymbol{\tau}$ at L_1' (Case A)

Figure 9 shows the time histories of E_a, E_w and W_J that are calculated for the optimal motion at L_1' in Case A. Around the start time, almost all the work W_J is stored in the robot arm as E_a as mentioned above. After that, a part of E_a is transmitted to E_w, and the ratio of E_w to W_J increases. In our opinion, this energy transmission would yield the peak of $\ddot{y}_e$ around $t = 0.1$ in Fig. 4.

C. Discussion

In V-A, we showed that W_J is maximized at the singular configurations by choosing $\boldsymbol{\tau}$ as $\boldsymbol{\tau} \parallel \boldsymbol{c}_\alpha$. In addition, when the robot base is located at the singular location S_1, the robot arm can pull the weight along y axis around the start time, because $\delta \boldsymbol{p}_e$ can be expressed as $[O(\delta\theta^3), O(\delta\theta^2)]^T$ for $\boldsymbol{\tau} \parallel \boldsymbol{c}_\alpha$. In the results in Case A and B, the optimal location L_1' is a little away from y axis. One reason for that would be that the location suitable to decelerate the weight around the end time is different from S_1. Moreover, the advantage of singular configurations shown in V-A are effective only for a heavy weight. For example, when $m_w = 0$ in Case A, the optimal location is obtained at $(x_b, y_b) = (-0.05, 0.35)$.

In the door opening problem dealt with in [11], the path of the end effector coincides with the path of the door knob, and the path does not have to be controlled by joint torque $\boldsymbol{\tau}$. As a result, the only task for joint torque $\boldsymbol{\tau}$ is supplying energy to the system, and we could see that $\boldsymbol{\tau} \parallel \boldsymbol{c}_0$ near $\mathcal{C}_0$ in [11]. On the other hand, in the problem dealt with in this paper, $\boldsymbol{\tau}$ has to not only supply energy to the system, but also control the path of the weight. Figure 10 shows the components of $\boldsymbol{\tau}$ along $\boldsymbol{e}_{\lambda_1}$ and $\boldsymbol{e}_{\lambda_2}$ for $\boldsymbol{\tau}$ shown in Fig. 5. Even at the start time, $\boldsymbol{\tau}$ has a component along $\boldsymbol{e}_{\lambda_2}$ to control the motion of the weight. Nevertheless, it is verified in Case A that the advantage of singular configurations in supplying energy is useful for minimizing the cost function. This advantage could be applied to a wide range of tasks that a robot arm is expected to do.

In Case B, the equations of motion in (6) include $\boldsymbol{\tau}_g$ because of the gravity. The optimal location L_1' in Case B is also close to the singular location S_1. If the robot base is located at S_1, $\boldsymbol{\tau}_g$ is eliminated and the robot arm is in the singular configuration $\mathcal{C}_0$, at the start time. However, joint torques necessary to achieve the tasks depend largely on $\boldsymbol{\tau}_g$ during the whole motion of the tasks. Further analysis of the dynamics is required to examine the advantage of singular configurations in detail under the force of gravity. An interesting thing in Case B is that the cost function has a local minimum at L_2 where the initial configuration of the robot arm is near $\mathcal{C}_\pi$. When we lift a heavy weight up to the height of our shoulder, the arm motion seems to connect $\mathcal{C}_0$ to $\mathcal{C}_\pi$ approximately. If the weight is lifted higher, the arm configuration returns to $\mathcal{C}_0$ from $\mathcal{C}_\pi$ again, like a weightlifting.

VI. Conclusions

In this paper, we showed that singular configurations of a two-link robot arm is useful in minimizing joint torques for tasks of pulling or lifting a heavy object. At the singular configurations, the energy is supplied more efficiently to the system by joint torques than at the other configurations. The singular configuration where the arm is stretched out has a better supply rate than the singular configuration where the arm is folded completely.

References

[1] H. Arisumi and J.-R. Chardonnet, "Dynamic Lifting Motion of Humanoid Robots," *Proc. of IEEE Conference on Robotics and Automation*, 2007, pp. 2661-2667

[2] D. Berenson, J. Kuffner and H. Choset, "An Optimization Approach to Planning for Mobile Manipulation," *Proc. of IEEE Conference on Robotics and Automation*, 2008, pp. 1187-1192

[3] J. P. Puga and L. E. Chiang, "Optimal Trajectory Planning for a Redundant Mobile Manipulator with Non-holonomic Constraints Performing Push-Pull Tasks," *Robotica*, vol. 26, pp. 385-394, 2008

[4] T. Yoshikawa, "Manipulability of Robotic Mechanisms," *The International Journal of Robotics Research*, vol. 4, no. 2, pp. 3-9, 1985

[5] M. Sampei and K. Furuta, "Robot Control in the Neighborhood of Singular Points," *IEEE Journal of Robotics and Automation*, vol. 4, no. 3, pp. 303-309, 1988

[6] D. N. Nenchev, Y. Tsumaki and M. Uchiyama, "Singularity-Consistent Parameterization of Robot Motion and Control," *The International Journal of Robotics Research*, vol. 19, no. 2, pp. 159-182, 2000

[7] K. Nagatani, T. Hirayama, A. Gofuku and Y. Tanaka, "Motion Planning for Mobile Manipulator with Keeping Manipulability," *Proc. of IEEE/RSJ International Conference on Intelligent Robots and Systems*, 2002, pp. 1663-1668

[8] T. Yoshikawa, "Dynamic Manipulability of Robot Manipulators," *Proc. of IEEE Conference on Robotics and Automation*, 1985, pp. 1033-1038

[9] V. Kumar and J. F. Gardner, "Kinematics of Redundantly Actuated Closed Chains," *IEEE Trans. on Robotics and Automation*, vol. 6, no. 2, pp. 269-274, 1990

[10] O. Khatib, "A Unified Approach for Motion and Force Control of Robot Manipulators: The Operational Space Formulation," *IEEE Journal of Robotics and Automation*, vol. 3, no. 1, pp. 43-53, 1987

[11] T. Urakubo, T. Mashimo and T. Kanade, "Optimal Placement of a Two-Link Manipulator for Door Opening," *Proc. of IEEE/RSJ International Conference on Intelligent Robots and Systems*, 2009, pp. 1446-1451